

# Influence of Disorder and Anharmonic Fluctuations on the Dynamical Rashba Effect in Purely Inorganic Lead-Halide Perovskites

Arthur Marronnier,<sup>\*,†</sup> Guido Roma,<sup>‡</sup> Marcelo Carignano,<sup>¶</sup> Yvan Bonnassieux,<sup>†</sup>  
Claudine Katan,<sup>§</sup> Jacky Even,<sup>||</sup> Edoardo Mosconi,<sup>⊥</sup> and Filippo De Angelis<sup>⊥,#</sup>

<sup>†</sup>*LPICM, CNRS, Ecole Polytechnique, Université Paris-Saclay, 91128 Palaiseau, France*

<sup>‡</sup>*DEN - Service de Recherches de Métallurgie Physique, CEA, Université Paris-Saclay,  
91191 Gif sur Yvette, France*

<sup>¶</sup>*Qatar Environment and Energy Research Institute, Hamad Bin Khalifa University, P.O.  
Box 5825, Doha, Qatar*

<sup>§</sup>*Univ Rennes, ENSCR, INSA Rennes, CNRS, ISCR (Institut des Sciences Chimiques de  
Rennes) – UMR 6226, F-35000 Rennes, France*

<sup>||</sup>*Univ Rennes, INSA Rennes, CNRS, Institut FOTON — UMR 6082, F-35000 Rennes,  
France*

<sup>⊥</sup>*Computational Laboratory for Hybrid/Organic Photovoltaics (CLHYO), CNR-ISTM, Via  
Elce di Sotto 8, I-06123 Perugia, Italy*

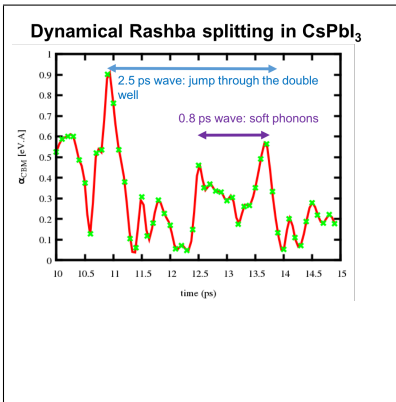
<sup>#</sup>*D3-CompuNet, Istituto Italiano di Tecnologia, Via Morego 30, 16163 Genova, Italy*

E-mail: arthur.marronnier@polytechnique.edu

## Abstract

Doping organic metal-halide perovskites with cesium could be the best solution to stabilize highly-efficient perovskite solar cells. The understanding of the respective roles of the organic molecule, on one hand, and the inorganic lattice, on the other, is thus crucial in order to be able to optimize the physical properties of the mixed-cation structures. In particular, the study of the recombination mechanisms is thought to be one of the key challenges towards full comprehension of their working principles. Using molecular dynamics and frozen phonons, we evidence sub-picosecond anharmonic fluctuations in the fully inorganic  $CsPbI_3$  perovskite. We reveal the effect of these fluctuations, combined with spin-orbit coupling, on the electronic band structure, evidencing a dynamical Rashba effect which could reduce recombination rates in these materials. Our study show that under certain conditions space disorder can quench the Rashba effect. As for time disorder, we evidence a dynamical Rashba effect which is similar to what was found for  $MAPbI_3$  and which is still sizable despite temperature disorder, the large investigated supercell, and the absence of the organic cations' motion.

## Graphical TOC Entry



## Keywords

inorganic perovskite solar cells, anharmonicity, cesium, phonons, DFT, molecular dynamics, Rashba

# Introduction

Fully inorganic metal-halide perovskites have attracted more and more attention in the past two years as they have showed promising efficiencies (record efficiency of 13.4% for quantum dot devices<sup>1</sup>) and as cesium doping has proven to be a good way to improve the environmental stability of hybrid metal-halide perovskites.<sup>2</sup> Moreover, a better understanding of the physical properties of fully inorganic halide perovskites is needed in order to further understand, by contrast, the role of the organic cation in their hybrid cousins.

In general, the enthusiasm for metal-halide perovskites can be explained by their exceptional optoelectronic properties, whether it be their optical properties,<sup>3-6</sup> the long lifetimes both electrons and holes<sup>7-9</sup> and the high mobility in these materials.<sup>9,10</sup> But what is probably the most remarkable feature of these materials is the fact that they present on the one hand good absorption and charge generation properties,<sup>11,12</sup> and very low recombination rates on the other hand. If the former could be explained in particular by the materials' direct band gap, the latter is more surprising as one should expect high values for both the radiative (direct band gap) and non-radiative recombination (high density of defects). As for defects, one should note that charge separation could be actually eased in these materials through halide ionic migration<sup>13,14</sup> which could either favour exciton screening<sup>15</sup> or give birth to local screening domains.<sup>16,17</sup>

This apparent paradox could potentially be explained by the consequences of the interplay of spin and orbital degrees of freedom, which are of important magnitude in these materials because of the presence of the heavy lead atoms. In particular, the giant spin-orbit coupling (SOC) that was reported in these materials<sup>18</sup> is expected to be at the origin of Rashba-like splittings.<sup>19-22</sup> Such splittings correspond to the lift of the electronic bands' spin degeneracy in the presence of SOC and time reversal symmetry when the inversion symmetry is broken in the crystal.<sup>23,24</sup> Assuming long-range polar distortions of the perovskite lattice, it can be shown that these band splittings can drastically impact the recombination rates by limiting direct transitions between the valence and conduction bands. This impact was theoretically

estimated by Zheng *et al.* to contribute to a reduction of the recombination rates reaching up to two orders of magnitude.<sup>8</sup> However, the existence of long-range polar distortions of iodide-based perovskite lattices is still debated, the influence of Rashba-like spinor band splittings could be more subtle and rather related to local lattice distortions.

Etienne *et al.*<sup>25</sup> investigated by DFT-based molecular dynamics the interplay of electronic and nuclear degrees of freedom in the prototype  $MAPbI_3$  perovskite and revealed a dynamical Rashba effect. They reported the influence of temperature and found a spatially local Rashba effect with fluctuations at the subpicosecond time scale, that is to say on the scale of the MA cation motion. It is worth pointing out that this numerical demonstration was based on MAPI structures preserving centrosymmetry on the average. They noticed that the Rashba splitting can be quenched when reaching room temperature but also when using larger supercells (up to 32 MAPI units, i.e., 3 nanometers cells) representing a higher and more realistic spatial disorder.

The local and dynamical nature of polar distortions may weaken the influence of Rashba-like spinor splittings by comparison to long range and static polar distortions. However the lack of long range correlations between local polar distortions could be compensated by the unusually strong amplitudes of the atomic motions. The strong anharmonicity of the perovskite lattice is a general feature of this new class of semiconductors,<sup>26</sup> that was pointed out experimentally very early by inelastic neutron scattering in the context of inorganic halide perovskites<sup>27</sup> and that shall give rise to at least two characteristic experimental signatures: large and anisotropic Debye-Waller factors in diffraction studies<sup>28,29</sup> and a so-called quasielastic central peak observed either in inelastic neutron or Raman scattering studies simultaneously with highly damped phonons.<sup>30,31</sup> However, the strong perovskite lattice anharmonicity is not expected to affect only zone center polar optical modes, but also acoustic modes or optical modes located at the edges or the Brillouin zone and related to non-polar antiferrodistortions.<sup>26</sup> The previously mentioned experimental signatures (Debye-waller factors, phonon damping and central peaks by inelastic neutron or Raman scattering studies)

can hardly be considered as unambiguous experimental proofs of the existence of strongly anharmonic polar fluctuations. Nowadays direct experimental investigations of the dielectric response give useful indications about the influence of lattice polar distortions<sup>32,33</sup> and the importance of the Fröhlich interaction<sup>34</sup> for electron-phonon coupling processes,<sup>35</sup> but do not directly probe the anharmonicity of polar distortions. Numerical simulations are therefore still useful tools that already allowed showing the presence of anharmonicity features in  $CsPbI_3$ ,<sup>36,37</sup> leading to symmetry breaking minimum structures in the high temperature phases both at the edges and at the center of the Brillouin zone. MD simulations for  $CsPbBr_3$  also suggested that the fluctuations in this material are mostly due to head-to-head Cs motion and Br face expansion happening on a few hundred femtosecond time scale.<sup>31</sup>

In that sense, large polar fluctuations of the perovskite lattice at the local scale may lead to two main effects: Rashba-like spinor splittings and strongly anharmonic polarons related to the Fröhlich interaction. We focus in the present contribution on the former aspect.

## Results and Discussion

In this article, we aim to further analyze the Rashba effect induced by the anharmonic double well and the symmetry breaking for the cubic phase of  $CsPbI_3$ . We have shown in our previous works<sup>36,37</sup> using the frozen phonon method that the highly symmetric cubic phase can be distorted to form two lower-symmetry structures with a slightly lower total energy (by a few meV). These two distorted structures, that we will call in the rest of the article  $A^+$  and  $A^-$ , have no inversion symmetry and correspond to the two minimum structures of the double well-instability recalled on Figure 1a.

They correspond to opposite distortions ( $\eta > 0$  and  $\eta < 0$ ) along the eigenmode represented in Figure 1b. Note that with rotational symmetry similar studies could be done on the two other eigenmodes corresponding to distortions along the two remaining Cartesian axes (y and z given our labeling).

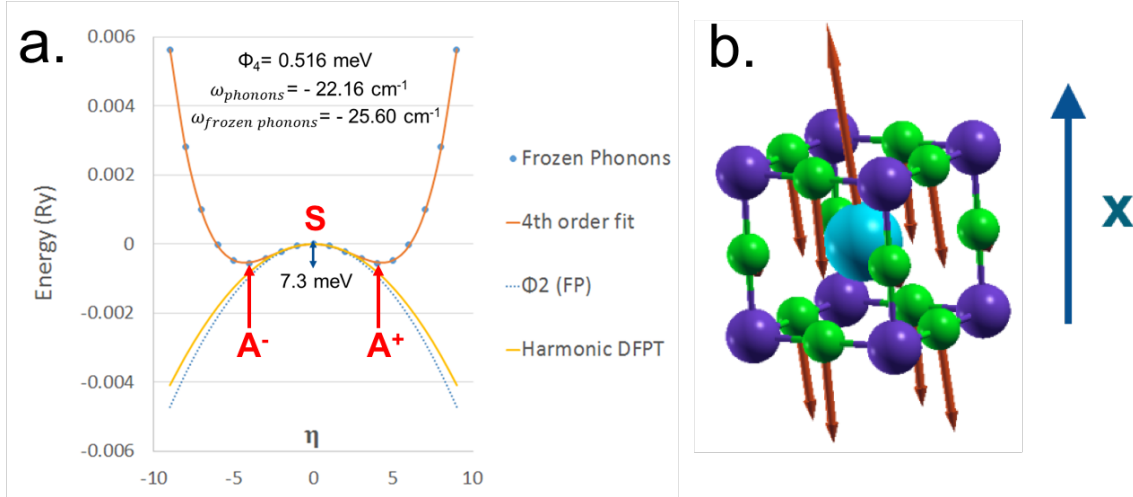


Figure 1: a. Potential energy surface from frozen phonon calculations of cubic  $CsPbI_3$  along the eigenvector of the unstable optical phonon at  $\Gamma$  (b) as a function of displacement parameter  $\eta$ . The  $3N$  dimensional displacement needed to reach the new minimum corresponds to around  $0.43\text{\AA}$ , including a  $0.36\text{\AA}$  displacement for the cesium atom. The blue, purple and green atoms respectively denote Cs, Pb and I. We chose to label as "x" the axis parallel to which this chosen distortion mostly occurs.  $\omega_{phonons}$  and  $\omega_{frozenphonons}$  represent the direct (DFPT) and frozen phonons estimations of the second derivative at  $\eta = 0$  (yellow and blue-dotted curve). For further details see Ref. 36.

The first aim of the study here is to look at the possible formation of " $A^+$  domains" and " $A^-$  domains", both in space (supercells) and in time (Car-Parrinello molecular dynamics "CPMD").

Then, we analyze in detail the dynamical Rashba effect induced by the time dynamics of the oscillations between structure  $A^+$  and structure  $A^-$  through the highly symmetric structure S ( $\eta = 0$ ). This study is done on CPMD trajectories obtained from Ref. 38

## Spatial disorder

First, the aim is to investigate the influence of spatial  $A^+/A^-$  domains on the electronic band structure, in particular in terms of Rashba effect. Given that the eigenvector under study mostly corresponds to a distortion along one axis (x as labeled in Figure 1b), we built supercells by doubling the single cell both in the x direction, and in the z direction.

These  $2 \times 1 \times 1$  and  $1 \times 1 \times 2$  supercells are built putting together 2 single cells: 1 single cell in configuration  $A^+$  (or x up), and one configuration in configuration  $A^-$  (or x down). These supercells, representing modulated structures with the smallest possible period, are schematically shown in Figure 2a.

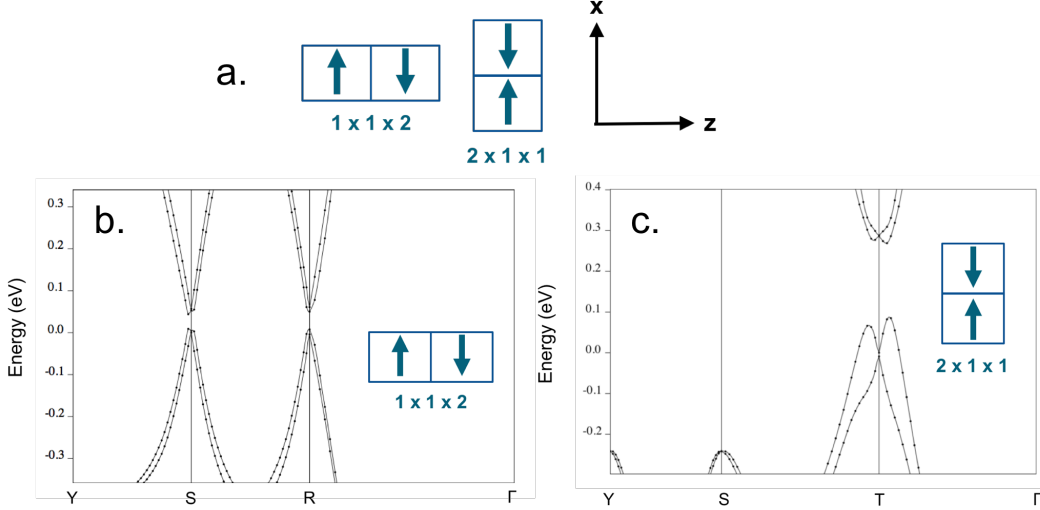


Figure 2: a. Simplified representations of the supercells used to study the influence of spatial domains  $A^+/A^-$  or "x up"/"x down" on the electronic band structure. Electronic band structure (including SOC) of the (b)  $1 \times 1 \times 2$  supercell and (c)  $2 \times 1 \times 1$  supercell. As the cell is slightly orthorhombic (see the Methods section), we use here the orthorhombic q-point convention.c.

The Rashba splitting obtained at the R point for a single cubic cell, in the minimum, symmetry-breaking structure is shown in Figure 3. When doubling the cell along z (resp. x), the R point folds onto the S point (resp. T point), using the orthorhombic convention. For this ordered, static reference we find energy splittings of 57 meV and 40 meV between the  $\Gamma$  point and respectively the conduction band minimum and valence band maximum. In order to give an estimate of the Rashba splitting taking into account the effect both in energy and in the k-space, we calculated the commonly used  $\alpha$  parameter as defined in Ref. 25:

$$\alpha_{C,V} = \frac{\Delta E_{C,V}}{2\Delta k_{C,V}} \quad (1)$$



where  $\Delta E_{C,V}$  is the energy difference between the first (resp. last) two bands of the conduction (resp. valence) bands and  $\Delta k_{C,V}$  the splitting of the minimum (resp. maximum) in the k-space. For the reference static, highly ordered structure we found  $\alpha$  values of 4.09 eV.Å and 2.01 eV.Å for respectively the conduction and the valence bands. These values are comparable to those in Ref. 25 in the case of polar  $MAPbI_3$ : 3.17 eV.Å and 1.17 eV.Å respectively. Note that so far the highest values found in ferroelectric materials for the Rashba parameter are 4.2-4.8 eV.Å for GeTe.<sup>39,40</sup>

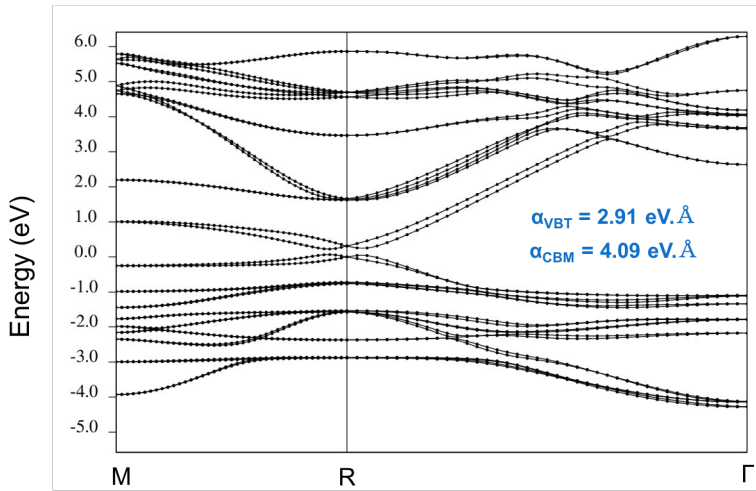


Figure 3: Electronic band structure (including SOC) of the unit cell of cubic  $CsPbI_3$ .

The results for the two modulated structures are shown in Figures 2b and 2c. Whereas no Rashba effect is found in the case of a modulation orthogonal to the direction of symmetry breaking, a band splitting around the valence band maximum and the conduction band minimum is found for a modulation parallel to the direction of symmetry breaking. We found  $\alpha$  values of 0.58 eV.Å and 2.18 eV.Å for the conduction and valence bands respectively.

In general, the Rashba splitting in the band structure of a two-dimensional system results from the combined effect of atomic spin-orbit coupling and asymmetry of the potential in the direction (here x) perpendicular to the two-dimensional plane, causing a loss of inversion symmetry. In the case of a modulation orthogonal to the direction of symmetry breaking ( $1 \times 1 \times 2$  supercell), the symmetry along x is respected on average: the inversion symmetry

is kept and the Rashba splitting is quenched. We expect then that the quenching of the Rashba effect results from a competition between parallel and orthogonal modulations: the former keeps the Rashba effect, while the latter tends to cancel it.

## Dynamical structural fluctuations

Next, we analyze in detail CPMD trajectories of cubic  $CsPbI_3$  in the light of our findings on the double well potential energy surface. The trajectories were computed by Carignano *et al.* in the framework of a study<sup>38</sup> of the anharmonic motion of the iodine atoms in  $CsPbI_3$  and  $MAPbI_3$ , where they showed that, at variance with  $FAPbI_3$ , these two perovskite structures are expected to have a deviation from the perfect cubic unit cell at any time of the MD, with a probability very close to 1. This hints towards the interpretation that the  $Pm\bar{3}m$  symmetry can be seen as a time average, including for  $CsPbI_3$ . This phenomenon had already been reported for  $MAPbI_3$  in earlier studies,<sup>17</sup> where it was evidenced that the system strongly deviates from the perfectly cubic structure in the sub-picosecond time scale.

The molecular dynamics simulation were performed at 370 K under NPT-F conditions, which allow volume fluctuations by changing the supercell edges and angles. The temperature was controlled by a Nose-Hoover thermostat with three chains, and the pressure was controlled by the Martyna's barostat.<sup>41</sup> The time constant for both, the thermostat and barostat, was set at 50 fs. The system they used for  $CsPbI_3$  has 320 atoms ( $4\times 4\times 4$  supercells).

In Figures 4a we show the lattice parameters fluctuations versus time. In particular, from this first simple analysis we can infer that the structure fluctuates around a cubic structure: the difference between the lattice parameters stays below 3%. Even though the structure is not perfectly cubic on average (see Table 1), the distance to the average pseudocubic lattice structure (Figure 4b) is smaller than 1%. This distance  $d$  is obtained as:

$$d(t) = \left( \sum_{i=1}^3 (x_i(t) - \bar{x}_i)^2 \right)^{\frac{1}{2}} \quad (2)$$

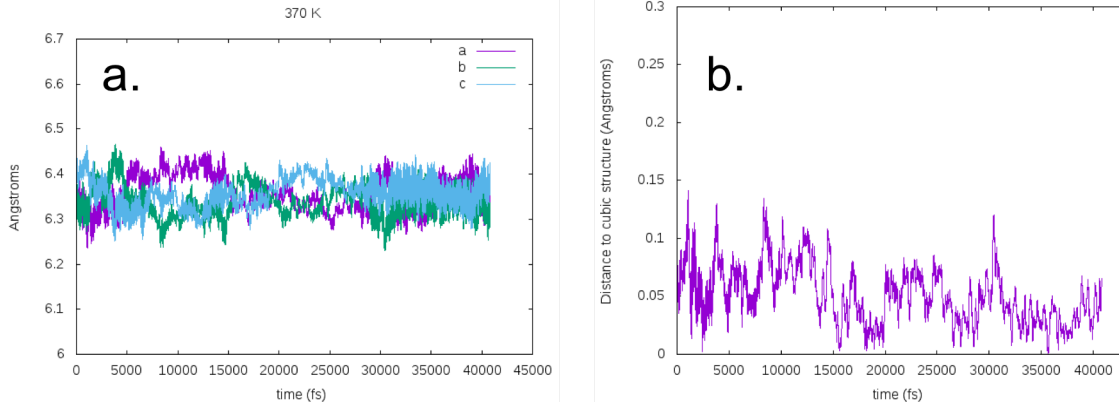


Figure 4: a. Lattice parameters fluctuations along the CPMD trajectory at 370 K. b. Fluctuations of the distance to the average pseudocubic structure, as defined in Eq. 2.

where  $x_i$  are the 3 lattice parameters and  $\bar{x}_i$  their time average over the whole trajectory.

**Table 1: Average lattice parameters (in Angstroms) along the CPMD trajectories at 370 K and 450 K.**

In Angstroms	370 K	450 K
a	6.358	6.372
b	6.338	6.391
c	6.358	6.361

In order to analyze the MD trajectories in the light of the aforementioned double well instability, we project these trajectories onto two kind of structures: the perfectly cubic symmetric structure ("S") and the symmetry breaking structures  $A^+$  and  $A^-$ . The chosen approach is to study the radial distribution function of the cesium-lead pairs during the MD simulation and to compare it to our two reference structures.

Figure 5 focuses on averages over 0.5 ps intervals. At this time scale, our double well references seem to explain very well how the system explores the energy landscape. Whereas some intervals show a distance peak corresponding to the distance in the average pseudocubic structure S, for instance the [11-11.5 ps] interval show two peaks centered on both minimum structures  $A^+$  and  $A^-$ . This means that within 0.5 ps the structure has enough time to explore the whole double well. We think that this is the most appropriate time-scale to

evidence the double well instabilities.

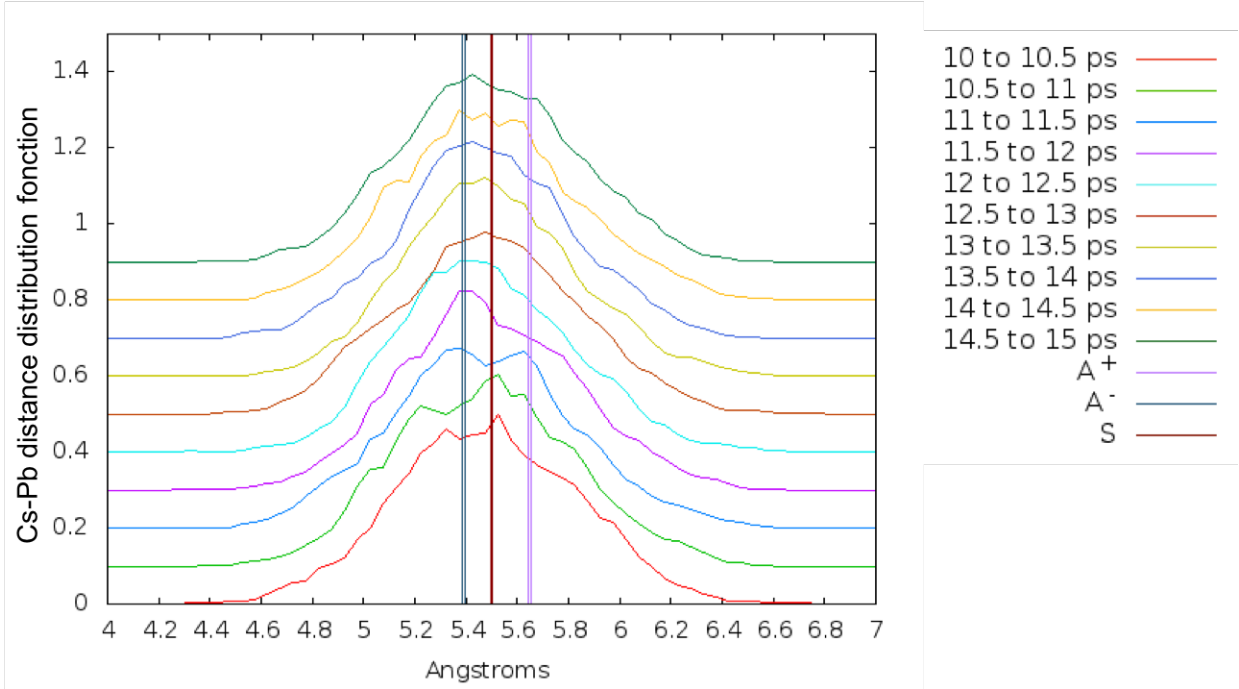


Figure 5: Distribution function of the cesium-lead pairs’ distances along the MD trajectory. Here the references (vertical lines) correspond to the distances for structures S,  $A^+$  and  $A^-$ , weighted by the ratio between the lattice parameters.

## Dynamical Rashba effect

We now focus on the dynamical Rashba effect possibly ensuing from the nuclear dynamics exposed above. We expect to find in  $CsPbI_3$  an effect similar to what was evidenced for  $MAPbI_3$  for which the spatially local Rashba splitting was found to fluctuate on the subpicosecond time scale typical of the methylammonium cation dynamics.<sup>25</sup>

To investigate this effect, we calculate the electronic band structure, including spin-orbit coupling, at different snapshots along the trajectory. Given the results of the Pb-Cs distance analysis, we chose to focus these calculations on the [10-15 ps] interval in which we chose 50 regularly distributed snapshots (hence separated by 100 fs from each other)

in order to better capture the sub pico-second dynamics. For each snapshot, we used the MD structure of the  $4 \times 4 \times 4$  supercells (we remind the reader that the cell's atomic positions, lattice parameters and angles vary) and derived its electronic band structure (see the Methods section). These calculations for  $4 \times 4 \times 4$  supercells follow the guidelines of those previously done for  $MAPbI_3$ .<sup>17</sup>

The electronic band structure calculations are done at 7 q points of the Brillouin zone (Table 2).

**Table 2: q points of the Brillouin zone used in the 50 band structure calculations in units of  $\frac{2\pi}{a_{x,y,z}^i}$  where  $a_{x,y,z}^i$  are the lattice parameters for snapshot i in one of the three cartesian direction, x, y or z.**

Point number	x	y	z
1	0.1	0	0
2	0.05	0	0
3 ( $\Gamma$ )	0	0	0
4	0	0.05	0
5	0	0.1	0
6	0	0	0.05
7	0	0	0.1

In Figure 6 we plot for each snapshot i of the 50 structures chosen in the MD trajectory and for each q point the normalized energy difference :

$$\Delta E_{gap}^i(q) = [CBM^i(q) - VBT^i(q)] - [(CBM^i(\Gamma) - VBT^i(\Gamma))] \quad (3)$$

where CBM is the conduction band minimum and VBT the valence band top. This is necessary as the cell is variable along the trajectory: the fluctuations on the gap value, which are large with respect to the Rashba splitting, would mask it otherwise.

These results show that 100 fs is a good estimate of the timescale of the Rashba effect dynamics. Moreover, on average we see a band gap shift to the Y direction, the band gap being reduced by 1.3 meV on average. Taking the extreme case, we can infer that the amplitude of the oscillations in the 5 ps timescale is around 10 meV.

Figures S1 and S2 show that this is mostly due to a Rashba splitting happening at the CBM rather than at the VBT. This is coherent with the fact that the most relativistic atom, Pb, is mostly contributing to the conduction band. This is coherent with what was previously reported for MAPI.<sup>17</sup>

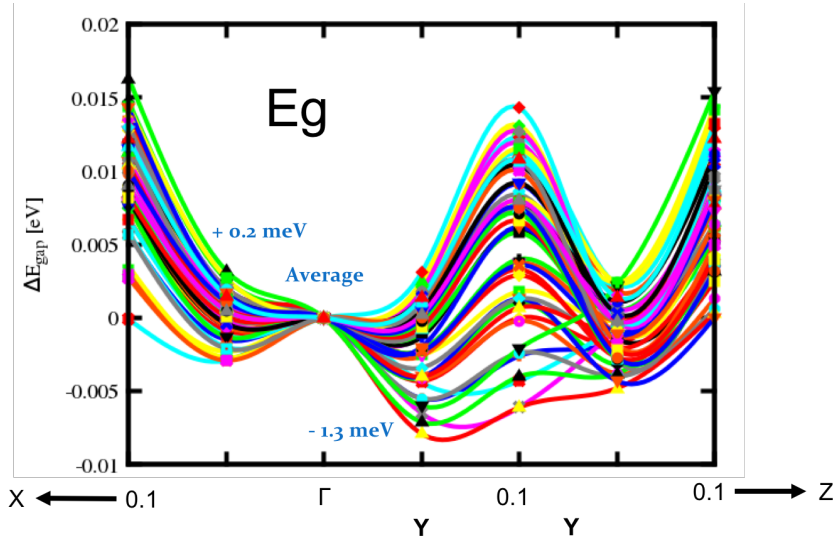


Figure 6: Differences between the gap at finite  $q$  and at  $\Gamma$  for the 50 snapshots chosen along the MD trajectory. This difference is 0 at  $\Gamma$  by construction (see Eq. 3). The Figures in blue represent the average values over the 50 points of the trajectory.

Figure 7a represent the Rashba effect oscillations in this interval through the previously defined  $\alpha$  parameter. This result confirms that the Rashba effect is much more substantial for the conduction band than for the valence bands, and oscillates with values close to  $1 \text{ eV} \cdot \text{\AA}$ . Even though this is smaller than in the static case (values around  $4 \text{ eV} \cdot \text{\AA}$ ), this means that the effect is still sizable despite the disorder induced by temperature and the large investigated supercell.

It is interesting to further look into these oscillations through a Fourier analysis (Figure 7b) which revealed the existence of two main frequency components :

- A 2.5 ps component which could correspond to the jump through double well and thus to the Cs slow motion

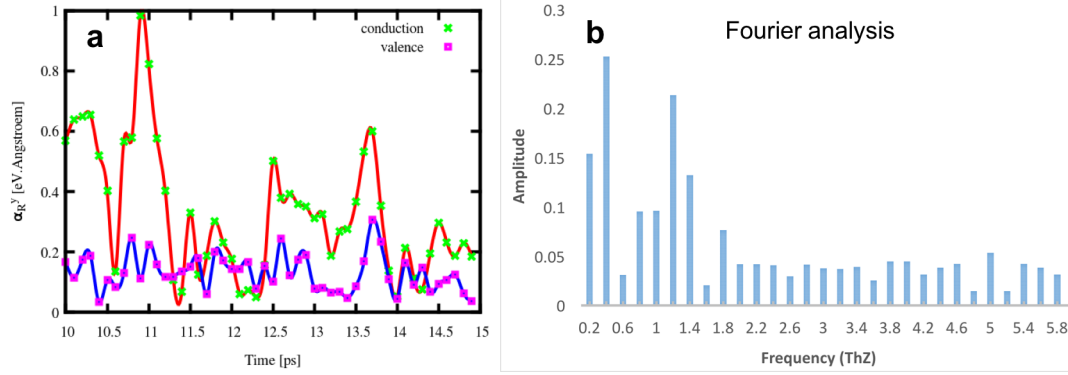


Figure 7: a.  $\alpha$  parameter for the conduction and valence bands versus time. b. Fourier analysis of  $\alpha$ 's oscillations.

- A 0.8 ps component corresponding to the phonon modes usually associated to the Pb-I stretching (around 20-40  $cm^{-1}$ )

We think it is of interest to compare the order of magnitudes of these oscillations to those obtained in a similar study lead on hybrid perovskite  $MAPbI_3$  by Etienne *et al.*<sup>25</sup> We report in Table 3 the corresponding values for the apolar structure of Ref. 25, because Cs atom has no permanent dipole moment. Note that nevertheless, for the polar structure, the largest  $\alpha$  value reported in Ref. 25 is even smaller (10.36). One needs to keep in mind that we have here very large supercells compared to what was used in that study. The conclusion we can draw from this comparison is that we observe a sizable dynamical Rashba effect even with large supercells and the absence of the organic molecule, which in general is a possible source of symmetry breaking in these halide perovskite structures.

**Table 3: Maximum value of the  $\alpha$  oscillations.**

Number of formula units	$\alpha$ for hybrid MAPI from Ref. 25 (eV.Å)	$\alpha$ for inorganic $CsPbI_3$ from our results (eV.Å)
1	12.48	
4	3.86	
32	2.19	
64		0.96

# Methods

## Density functional theory for band structure calculations

In this study we used for the minimum reference structures the ones obtained in Ref<sup>36</sup> after relaxation performed with LDA (cutoff of 70 Ry) letting both the lattice parameters and the atomic positions relax, keeping the cell's angles fixed. These structures are thus slightly orthorhombic (0.1 and 0.3 % distortion). **The total energy of these relaxed structures is 11.3 meV under the maximum, high-symmetry cubic structure. (If the angles are not constrained, the energy difference reads 12.1 meV).**

For these reference structures, geometry optimizations and force calculations were performed with the Local Density Approximation (LDA). Non-relativistic (scalar-relativistic for Pb) and norm-conserving pseudopotentials were used, with the Cs [ $5s^25p^66s^1$ ], I [ $5s^25p^5$ ] and Pb [ $5d^{10}6s^26p^2$ ] electrons treated as valence states. The choice of 14 electrons for Pb and 9 for Cs was made after testing the influence of semi-core electrons on the potential energy surface (see an example in Figure 5 of our previous article<sup>36</sup>).

In a second step:

- as for the study of the spatial domains, the band structure calculations of the constructed  $2\times 1\times 1$  and  $1\times 1\times 2$  supercells were performed with fully relativistic pseudopotentials (for Pb and I) with LDA.
- in order to study the dynamical Rashba effect from CPMD, the band structure calculations were performed with fully relativistic US pseudopotentials (for Pb, I and Cs) datasets using the PBE xc functional (with the same number of valence electrons as in the scalar or non-relativistic case). This was done in order to be coherent with the CPMD calculations from which MD trajectories were taken,<sup>38</sup> which were done using PBE as well (with the CP2K code). We carefully checked that symmetry breaking is present even when using PBE, see Ref.<sup>37</sup>



For all the calculations, the Brillouin zone was sampled with  $\Gamma$ -centered Monkhorst-Pack meshes<sup>42</sup> with subdivisions of  $8\times 8\times 8$  k-points.

## Concluding remarks

In summary, we investigated the effect of spatial and temporal disorder on the Rashba splitting in the cubic  $\alpha$  phase of inorganic halide perovskite  $CsPbI_3$ . The analysis focused on the fluctuations of the Rashba  $\alpha$ -parameter—a measure of the Rashba band splitting—along a molecular dynamics trajectory for a large supercell.<sup>38</sup>

Our results highlight a dynamical Rashba effect similar to the one previously observed for hybrid organic-inorganic halide perovskites,<sup>25</sup> which persists in spite of the quenching effect coming from spatial disorder in this relatively large simulation cell (320 atoms).

Some low-frequency vibrational modes of the system, and in particular the anharmonic behavior, which has been shown to originate from the double well potential energy landscape of a polar optical phonon,<sup>36</sup> contribute to the spatial extension of the Rashba effect. This is confirmed by the Fourier analysis of the Rashba  $\alpha$ -parameter fluctuations.

An expected consequence of the Rashba effect is the reduction of the carriers recombination rate<sup>8</sup> and consequent enhancement of their lifetime ; therefore, our results are a promising piece of information for the applications of fully inorganic halide perovskite as photovoltaic devices.

## Associated Content

The authors declare no competing financial interest.

## Acknowledgement

Dr. Arthur Marronnier's PhD project was funded by the Graduate School of École des Ponts ParisTech and the French Department of Energy (MTES). HPC resources of TGCC and CINES were used through allocation 2017090642 and x20170906724 GENCI projects. The work at FOTON and ISCR was funded by the European Union's Horizon 2020 program, through a FET Open research and innovation action under the grant agreement No 687008.

## Supporting Information Available

The following files are available free of charge.

We provide in the supporting information additional results on the effect of dynamical disorder on the conduction band minimum and valence band top throughout the chosen 5 ps interval of study for our band structure calculations.

## References

- (1) Sanehira, E. M.; Marshall, A. R.; Christians, J. A.; Harvey, S. P.; Ciesielski, P. N.; Wheeler, L. M.; Schulz, P.; Lin, L. Y.; Beard, M. C.; Luther, J. M. Enhanced mobility CsPbI<sub>3</sub> quantum dot arrays for record-efficiency, high-voltage photovoltaic cells. *Science Advances* **2017**, *3*.
- (2) Saliba, M.; Matsui, T.; Seo, J.-Y.; Domanski, K.; Correa-Baena, J.-P.; Nazeeruddin, M. K.; Zakeeruddin, S. M.; Tress, W.; Abate, A.; Hagfeldt, A. et al. Cesium-containing Triple Cation Perovskite Solar Cells: Improved Stability, Reproducibility and High Efficiency. *Energy Environ. Sci.* **2016**, *9*, 1989–1997.
- (3) Chiarella, F.; Zappettini, A.; Licci, F.; Borriello, I.; Cantele, G.; Ninno, D.; Cassinese, A.; Vaglio, R. Combined experimental and theoretical investigation of optical,

- structural, and electronic properties of  $\text{CH}_3\text{NH}_3\text{SnX}_3$  thin films (X= Cl, Br). *Physical Review B* **2008**, *77*, 045129.
- (4) Ogomi, Y.; Morita, A.; Tsukamoto, S.; Saitho, T.; Fujikawa, N.; Shen, Q.; Toyoda, T.; Yoshino, K.; Pandey, S. S.; Ma, T. et al.  $\text{CH}_3\text{NH}_3\text{Sn}_x\text{Pb}_{1-x}\text{I}_3$  Perovskite solar cells covering up to 1060 nm. *The journal of physical chemistry letters* **2014**, *5*, 1004–1011.
- (5) Eperon, G. E.; Stranks, S. D.; Menelaou, C.; Johnston, M. B.; Herz, L. M.; Snaith, H. J. Formamidinium Lead Trihalide: a Broadly Tunable Perovskite for Efficient Planar Heterojunction Solar Cells. *Energy Environ. Sci.* **2014**, *7*, 982.
- (6) Stoumpos, C. C.; Malliakas, C. D.; Kanatzidis, M. G. Semiconducting Tin and Lead Iodide Perovskites with Organic Cations: Phase Transitions, High Mobilities, and Near-Infrared Photoluminescent Properties. *Inorg. Chem.* **2013**, *52*, 9019–9038.
- (7) Wehrenfennig, C.; Liu, M.; Snaith, H. J.; Johnston, M. B.; Herz, L. M. Charge-carrier dynamics in vapour-deposited films of the organolead halide perovskite  $\text{CH}_3\text{NH}_3\text{PbI}_{3-x}\text{Cl}_x$ . *Energy & Environmental Science* **2014**, *7*, 2269–2275.
- (8) Zheng, F.; Tan, L. Z.; Liu, S.; Rappe, A. M. Rashba spin–orbit coupling enhanced carrier lifetime in  $\text{CH}_3\text{NH}_3\text{PbI}_3$ . *Nano letters* **2015**, *15*, 7794–7800.
- (9) Ponseca Jr, C. S.; Savenije, T. J.; Abdellah, M.; Zheng, K.; Yartsev, A.; Pascher, T.; Harlang, T.; Chabera, P.; Pullerits, T.; Stepanov, A. et al. Organometal halide perovskite solar cell materials rationalized: ultrafast charge generation, high and microsecond-long balanced mobilities, and slow recombination. *Journal of the American Chemical Society* **2014**, *136*, 5189–5192.
- (10) Cahen, D.; Edri, E.; Hodes, G.; Gartsman, K.; Kirmayer, S.; Mukhopadhyay, S. Elucidating the charge carrier separation and working mechanism of  $\text{CH}_3\text{NH}_3\text{PbI}_{3-x}\text{Cl}_x$  perovskite solar cells. *Nature communications* **2014**, *5*, 3461.

- (11) Xing, G.; Mathews, N.; Sun, S.; Lim, S. S.; Lam, Y. M.; Grätzel, M.; Mhaisalkar, S.; Sum, T. C. Long-range balanced electron-and hole-transport lengths in organic-inorganic  $\text{CH}_3\text{NH}_3\text{PbI}_3$ . *Science* **2013**, *342*, 344–347.
- (12) Stranks, S. D.; Eperon, G. E.; Grancini, G.; Menelaou, C.; Alcocer, M. J.; Leijtens, T.; Herz, L. M.; Petrozza, A.; Snaith, H. J. Electron-hole diffusion lengths exceeding 1 micrometer in an organometal trihalide perovskite absorber. *Science* **2013**, *342*, 341–344.
- (13) Lee, H.; Gaiaschi, S.; Chapon, P.; Marronnier, A.; Lee, H.; Vanel, J.-C.; Tondelier, D.; Boureé, J.-E.; Bonnassieux, Y.; Geffroy, B. Direct Experimental Evidence of Halide Ionic Migration under Bias in  $\text{CH}_3\text{NH}_3\text{PbI}_{3-x}\text{Cl}_x$ -Based Perovskite Solar Cells Using GD-OES Analysis. *ACS Energy Letters* **2017**, *2*, 943–949.
- (14) Yang, T.-Y.; Gregori, G.; Pellet, N.; Grätzel, M.; Maier, J. The significance of ion conduction in a hybrid organic–inorganic lead-iodide-based perovskite photosensitizer. *Angewandte Chemie* **2015**, *127*, 8016–8021.
- (15) Even, J.; Pedesseau, L.; Katan, C. Analysis of multivalley and multibandgap absorption and enhancement of free carriers related to exciton screening in hybrid perovskites. *The Journal of Physical Chemistry C* **2014**, *118*, 11566–11572.
- (16) Ma, J.; Wang, L.-W. Nanoscale charge localization induced by random orientations of organic molecules in hybrid perovskite  $\text{CH}_3\text{NH}_3\text{PbI}_3$ . *Nano letters* **2014**, *15*, 248–253.
- (17) Quarti, C.; Mosconi, E.; Ball, J. M.; D’Innocenzo, V.; Tao, C.; Pathak, S.; Snaith, H. J.; Petrozza, A.; De Angelis, F. Structural and optical properties of methylammonium lead iodide across the tetragonal to cubic phase transition: implications for perovskite solar cells. *Energy Environ. Sci.* **2016**, *9*, 155–163.
- (18) Even, J.; Pedesseau, L.; Jancu, J.-M.; Katan, C. Importance of spin–orbit coupling

- in hybrid organic/inorganic perovskites for photovoltaic applications. *The Journal of Physical Chemistry Letters* **2013**, *4*, 2999–3005.
- (19) Kim, M.; Im, J.; Freeman, A. J.; Ihm, J.; Jin, H. Switchable  $S = 1/2$  and  $J = 1/2$  Rashba bands in ferroelectric halide perovskites. *Proceedings of the National Academy of Sciences* **2014**, *111*, 6900–6904.
- (20) Even, J.; Pedesseau, L.; Jancu, J.-M.; Katan, C. DFT and k-p Modelling of the Phase Transitions of Lead and Tin Halide Perovskites for Photovoltaic Cells. *Phys. Status Solidi RRL* **2014**, *8*, 31–35.
- (21) Amat, A.; Mosconi, E.; Ronca, E.; Quarti, C.; Umari, P.; Nazeeruddin, M. K.; Grätzel, M.; De Angelis, F. Cation-Induced Band-Gap Tuning in Organohalide Perovskites: Interplay of Spin–Orbit Coupling and Octahedra Tilting. *Nano Lett.* **2014**, *14*, 3608–3616.
- (22) Brivio, F.; Butler, K. T.; Walsh, A.; van Schilfhaarde, M. Relativistic quasiparticle self-consistent electronic structure of hybrid halide perovskite photovoltaic absorbers. *Phys. Rev. B* **2014**, *89*, 155204.
- (23) Zhang, X.; Liu, Q.; Luo, J.-W.; Freeman, A. J.; Zunger, A. Hidden spin polarization in inversion-symmetric bulk crystals. *Nature Physics* **2014**, *10*, 387.
- (24) Kepenekian, M.; Robles, R.; Katan, C.; Saponi, D.; Pedesseau, L.; Even, J. Rashba and Dresselhaus Effects in Hybrid Organic–Inorganic Perovskites: From Basics to Devices. *ACS Nano* **2015**, *9*, 11557–11567, PMID: 26348023.
- (25) Etienne, T.; Mosconi, E.; De Angelis, F. Dynamical Origin of the Rashba Effect in Organohalide Lead Perovskites: A Key to Suppressed Carrier Recombination in Perovskite Solar Cells? *J. Phys. Chem. Lett.* **2016**, *7*, 1638–1645.

- (26) Katan, C.; Mohite, A. D.; Even, J. Riddles in perovskite research. *Nature materials* **2018**, *17*, 377–384.
- (27) Fujii, Y.; Hoshino, S.; Yamada, Y.; Shirane, G. Neutron-scattering Study on Phase Transitions of CsPbCl<sub>3</sub>. *Phys. Rev. B* **1974**, *9*, 4549–4559.
- (28) Trots, D.; Myagkota, S. High-temperature Structural Evolution of Caesium and Rubidium Triiodoplumbates. *J. Phys. Chem. Solids* **2008**, *69*, 2520 – 2526.
- (29) Hutton, J.; Nelmes, R.; Meyer, G.; Eiriksson, V. High-resolution studies of cubic perovskites by elastic neutron diffraction: CsPbCl<sub>3</sub>. *Journal of Physics C: Solid State Physics* **1979**, *12*, 5393.
- (30) Even, J.; Carignano, M.; Katan, C. Molecular Disorder and Translation/Rotation Coupling in the Plastic Crystal Phase of Hybrid Perovskites. *Nanoscale* **2016**, *8*, 6222–6236.
- (31) Yaffe, O.; Guo, Y.; Tan, L. Z.; Egger, D. A.; Hull, T.; Stoumpos, C. C.; Zheng, F.; Heinz, T. F.; Kronik, L.; Kanatzidis, M. G. et al. Local polar fluctuations in lead halide perovskite crystals. *Physical review letters* **2017**, *118*, 136001.
- (32) Marronnier, A.; Lee, H.; Lee, H.; Kim, M.; Eypert, C.; Gaston, J.-P.; Roma, G.; Tondelier, D.; Geffroy, B.; Bonnassieux, Y. Electrical and Optical Degradation Study of Methylammonium-based Perovskite Materials under Ambient Conditions. *Sol. Energy Mater. Sol. Cells* **2018**, *178*, 179 – 185.
- (33) Anusca, I.; Balčiūnas, S.; Gemeiner, P.; Svirskas, Š.; Sanlialp, M.; Lackner, G.; Fettkenhauer, C.; Belovickis, J.; Samulionis, V.; Ivanov, M. et al. Dielectric response: Answer to many questions in the methylammonium lead halide solar cell absorbers. *Advanced Energy Materials* **2017**, *7*, 1700600.
- (34) Sendner, M.; Nayak, P. K.; Egger, D. A.; Beck, S.; Müller, C.; Epping, B.; Kowalsky, W.; Kronik, L.; Snaith, H. J.; Pucci, A. et al. Optical phonons in methylammonium lead

- halide perovskites and implications for charge transport. *Mater. Horiz.* **2016**, *3*, 613–620.
- (35) Fu, M.; Tamarat, P.; Trebbia, J.-B.; Bodnarchuk, M. I.; Kovalenko, M. V.; Even, J.; Lounis, B. Unraveling exciton–phonon coupling in individual FAPbI<sub>3</sub> nanocrystals emitting near-infrared single photons. *Nature communications* **2018**, *9*, 3318.
- (36) Marrognier, A.; Lee, H.; Geffroy, B.; Even, J.; Bonnassieux, Y.; Roma, G. Structural Instabilities Related to Highly Anharmonic Phonons in Halide Perovskites. *J. Phys. Chem. Lett.* **2017**, *8*, 2659–2665.
- (37) Marrognier, A.; Roma, G.; Boyer-Richard, S.; Pedesseau, L.; Jancu, J.-M.; Bonnassieux, Y.; Katan, C.; Stoumpos, C. C.; Kanatzidis, M. G.; Even, J. Anharmonicity and Disorder in the Black Phases of Cesium Lead Iodide Used for Stable Inorganic Perovskite Solar Cells. *ACS Nano* **2018**, PMID: 29565559.
- (38) Carignano, M. A.; Aravindh, S. A.; Roqan, I. S.; Even, J.; Katan, C. Critical Fluctuations and Anharmonicity in Lead Iodide Perovskites from Molecular Dynamics Supercell Simulations. *The Journal of Physical Chemistry C* **2017**, *121*, 20729–20738.
- (39) Picozzi, S. Ferroelectric Rashba semiconductors as a novel class of multifunctional materials. *Frontiers in Physics* **2014**, *2*, 10.
- (40) Krempaský, J.; Volfová, H.; Muff, S.; Pilet, N.; Landolt, G.; Radović, M.; Shi, M.; Kriegner, D.; Holý, V.; Braun, J. et al. Disentangling bulk and surface Rashba effects in ferroelectric  $\alpha$ -GeTe. *Phys. Rev. B* **2016**, *94*, 205111.
- (41) Martyna, G. J.; Tuckerman, M. E.; Tobias, D. J.; Klein, M. L. Explicit reversible integrators for extended systems dynamics. *Molecular Physics* **1996**, *87*, 1117–1157.
- (42) Monkhorst, H. J.; Pack, J. D. Special points for Brillouin-zone integrations. *Physical review B* **1976**, *13*, 5188.